의학박사 학위논문

Histopathologic study for healing of aneurysm after flow diverter stenting in canine model

개의 모델에서 혈류전환 스텐트에 의한 동맥류 치료과정의 조직병리학적 연구

2017년 2월

서울대학교 대학원

의학과 영상의학 전공

이 종 영

의학박사 학위논문

Histopathologic study for healing of aneurysm after flow diverter stenting in canine model

개의 모델에서 혈류전환 스텐트에 의한 동맥류 치료과정의 조직병리학적 연구

2017년 2월

서울대학교 대학원

의학과 영상의학 전공

이 종 영

Histopathologic study for healing of aneurysm after flow diverter stenting in canine model

지도교수 한 문 희

이 논문을 의학박사학위논문으로 제출함

2016년 9월

서울대학교 대학원

의학과 영상의학 전공

이 종 영

이종영의 박사학위논문을 인준함

2017년 1월

위 원 장 _____ (인)

부 위 원 장 _____ (인)

위 원 _____ (인)

위 원 _____ (인)

위 원 _____ (인)

Histopathologic study for healing of aneurysm after flow diverter stenting in canine model

By

Jong Young Lee

A Thesis Submitted to the Department of Radiology in Partial Fulfillment

of the Requirement for the Degree of Doctor of Philosophy

in Medicine at the Seoul National University College of Medicine

September 2016

Approved by thesis committee

January 2017

Abstract

Histopathologic study for healing of aneurysm after flow diverter stenting in canine model

Jong Young Lee
Department of Radiology
College of Medicine
The Graduate School
Seoul National University

Flow diverters (FDs) have been used widely for the treatment of intracranial aneurysms, showing good clinical results even in large and giant aneurysms. However, the exact healing mechanism associated with FDs remains poorly understood. The purpose of this study is to describe the healing process of aneurysms treated using a flow diverter by demonstrating the histopathologic progression in a canine aneurysm model. With institutional animal care and use committee approval, 24 side wall aneurysms were created in the common carotid artery of 8 dogs. All of 24 aneurysms were remained patently, and 21

of 24 aneurysms were used for FD deployment. Aneurysms were treated with two different flow diverters, 48- and 32-strand. Angiographic follow-up was performed immediately after placement of the device and at 4- and 12-weeks post treatment. At last follow-up, the aneurysm and the device-implanted parent artery were harvested. Angiographic findings revealed that the 48-strand flow diverter achieved a higher occlusion rate compared to the 32-strand flow diverter. Histopathologic examination of aneurysms with complete and near-complete occlusion at 4 weeks follow-up showed the development of intra-aneurysm thrombus formation in a laminating fashion, and neointimal thickening at the mid-segment of the aneurysm. The degree of thrombus formation and organization was variable, and the size of the aneurysmal sac also varied. At 12 weeks, examinations showed markedly shrunken aneurysmal sacs filled with organized connective tissue with a thin neointima. In aneurysms with incomplete occlusion at 4 weeks, aneurysmal sacs were most commonly filled with a multi-staged thrombus composed primarily of fresh blood clot with or without an empty space with neointimal thickening at

the mid-segment of the aneurysm. At 12 weeks, examination showed a small amount of organized thrombus around the fringe neck and a large empty space with thick neointimal formation. Neointimal thickness was not significantly different between the two treatment groups or between the two follow-up periods. Among aneurysms showing the same angiographic outcomes at a specific follow-up period, various degrees and patterns of intra-aneurysmal thrombus formation with different sized aneurysm sacs were found. In conclusion, angiographic outcome could not represent a degree of aneurysm healing after FD deployment. Neointimal formation could occur along the struts of the FD independently of intra-aneurysmal thrombus formation. However, neointima formation could not solely lead to complete aneurysm healing. Intra-aneurysmal thrombus formation and organization seems to be an important factor for the complete occlusion of aneurysms treated using the FD.

Key words: Aneurysm, Flow diverter, Histopathology, Canine model
Student number: 2010-30540

List of Tables

Table 1. Flow diverter profiles ---------- 9

Table 2. Aneurysm description by duration with 32-strand and 48-strand flow diverter stent ---------- 19

Table 3-1. Angiographic outcomes of aneurysms treated with 32-strand flow diverters---------- 22

Table 3-2. Angiographic outcomes of aneurysms treated with 48-strand flow diverters ---------- 23

Table 4-1. Angiographic outcomes and histopathologic findings at 4-week follow-up ---------- 33

Table 4-2. Angiographic outcomes and histopathologic findings at 4-week follow-up ---------- 34

Table 4-3. Angiographic outcomes and histopathologic findings at 4-week follow-up ---------- 35

Table 5-1. Angiographic outcomes and histopathologic findings at 12-week follow-up ---------- 36

Table 5-2. Angiographic outcomes and histopathologic findings at 12-week follow-up ---------- 37

List of Figures

Figure 1. Schematic diagram of four side-wall aneurysms in a canine model and *in-situ* aneurysm ---------- 5

Figure 2. Schematic diagram of wire-braiding technology ---------- 6

Figure 3. Schematic diagram and image of the 32-strand flow diverter configuration ---------- 7

Figure 4. Intra-aneurysmal flow modification measure ---------- 12

Figure 5. Angiographic outcome measure ---------- 14

Figure 6. Morphometric measures of neointima, neolumen and former vessel lumen ---------- 16

Figure 7. Aneurysms of complete occlusion at 4-week follow-up -- 25

Figure 8. Aneurysms of grade III occlusion at 4-week follow-up - 27

Figure 9. Aneurysms of incomplete occlusion at 4-week follow-up - 28

Figure 10. Aneurysms of complete and grade III occlusion at 12-week follow-up---------- 30

Figure 11. Aneurysm of incomplete occlusion at 12-week follow-up-31

List of abbreviation

FD (flow diverter)

IACUC (Institutional Animal Care and Use Committee)

CCA (common carotid artery)

SCA (subclavian artery)

VA (vertebral artery)

DSA (digital subtraction angiography)

PPI (pore per inch)

PED (Pipeline embolization device)

MMA (methyl-metacrylate)

Contents

I. Introduction ---------- 1

II. Materials and methods ---------- 3

III. Results ---------- 18

IV. Discussion ---------- 38

V. Conclusion ---------- 47

VI. References ---------- 48

VII. Abstract (국문초록) ---------- 55

I. INTRODUCTION

Flow diverters (FDs) have been used widely for the treatment of intracranial aneurysms, showing good clinical results even in large and giant aneurysms.[1-7] However, the exact healing mechanism associated with FDs remains poorly understood. To evaluate the healing process, numerous *ex-vivo* and/or *in-vivo* experimental studies have been performed, most commonly focused on the relationship between the degree of hemodynamic alteration induced by different types of FDs and their efficacy.[8-13] Some *in-vivo* experimental studies demonstrated the aneurysm healing process, emphasizing neointima formation by measuring various biomarkers.[14, 15] Even though these data provide useful information for the understanding of the aneurysm healing mechanism with FDs, there are some limitations to our comprehension of the overall aneurysm healing process.

In clinical practice, angiographic findings were used as an outcome measure for an efficacy of FD to treat an aneurysm. According to the angiographic outcomes, we usually suspect the degree of aneurysm healing

after FD deployment. It presumed that aneurysm healing process after FD deployment would be relatively homogenous depending on degrees of an angiographic outcome.

The aim of the present study was to describe the healing process of aneurysms treated using an FD by demonstrating the histopathologic progression in a canine side wall aneurysm model.

II. MATERIALS and METHODS

1. Animal experiments

All experimental protocols were approved by the Institutional Animal Care and Use Committee (IACUC) of Seoul National University Hospital (SNUH-IACUC No. 11-0001), and conducted in accordance with the animal experiment guidelines. Twenty-one wide-necked, side wall saccular aneurysms using a venous pouch were created in 8 morphologically normal male, mongrel dogs of similar size and weight (28 ~ 32 kg). Four aneurysms were created in 4 dogs as shown at figure 1-A, and two aneurysms, one at each side, were created in 4 dogs. Operations were performed under sterile conditions. After induction with intramuscular injection of 15mg/kg of Zoletil (zolazepam and tiletamine, Virbac AH, Fort Worth, TX, USA) and 10mg/kg of Rompun (xylazine, Bayer Animal Health GmbH, Germany), general endotracheal anesthesia was maintained using 1% to 3% inhaled isoflurane (Forane, Choongwae Pharma, Seoul, Korea) throughout the procedure. After that, paramedian, vertical skin incisions were made on the neck and the right

jugular vein was isolated and ligated proximally and distally. The surgeon prepared 5-8mm sections of the vein. One end of each venous segment was ligated using 3-0 black silk. The common carotid artery (CCA) was then isolated. Proximal and distal control of the CCA was achieved using temporary aneurysm clips. Elliptical arteriotomy, approximately 10 mm in length, was performed at the mid portion of the exposed artery. The open end of the prepared venous segment was sewn along the edge of the arteriotomy using 7-0 Proline sutures (Ethicon, Inc., Somerville, NJ) (Figure 1).

After meticulous hemostasis, the deep fascial tissues were sutured, followed by skin closure. Same procedures were performed at the contra-lateral side. After completion of survival procedures, the animals were given 2mg/kg of subcutaneous Ketoprofen (Ketoprofen, UniBiotech, Seoul, Korea) as analgesic, anti-inflammatory, and antipyretic immediately after surgery and twice daily for 3 days postoperatively. All aneurysms were checked using digital subtraction angiography (DSA) at 1 and 4 weeks after aneurysm creation using a mobile C-arm system (BV Pulsera, Philips Medical System,

The Netherland).

We used the aneurysm models as experimental subjects when the patency of the intra-aneurysmal and parent arterial flow was confirmed by 4-week conventional angiography.

A. 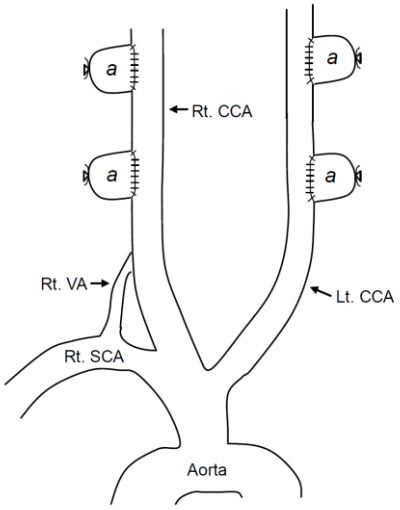

B. 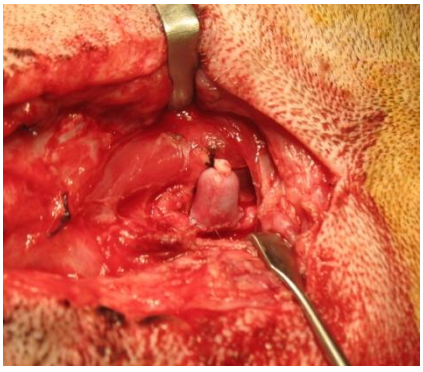

Figure 1. Schematic diagram of four side-wall aneurysms in a canine model and *in-situ* aneurysm.

A. *a* indicates venous pouch, side-wall aneurysm. CCA indicates common carotid artery; SCA, subclavian artery; and VA, vertebral artery. B. *in-situ* photograph of an aneurysm 8.

2. Flow diverter device

The devices were constructed of 0.002-inch nitinol wires and were self-expanding in nature. Stents (NOD stent, Access Point Technologies LLC, Roger, MN) were manufactured using an automated braiding machine (Steeger horizontal fine wire braider Model HS80, Steeger USA, Inman, SC). During the process, nitinol wires were knitted onto a cylindrically shaped mandrel in a controlled angle (Figure 2).

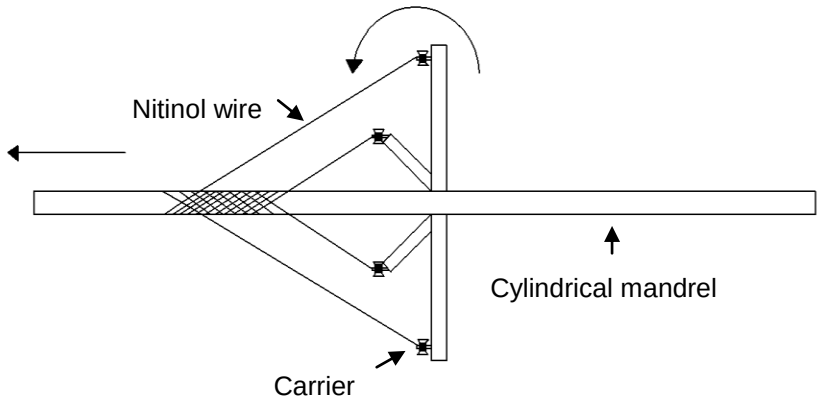

Figure 2. Schematic diagram of wire-braiding technology

In braiding, layers of helically wound nitinol wire are interlaced in a cylindrical shape, and interlocks can be produced at every intersection of nitinol wires. During the process, a cylindrical mandrel is fed through the center of a braiding machine at a uniform rate, and the nitinol wire from carriers is braided around the mandrel at a controlled angle.

The stent provides two types of section: a central portion, 1/3 of the stent length, with tight braiding distances and margins of smoother, wide interstices (Figure 3).

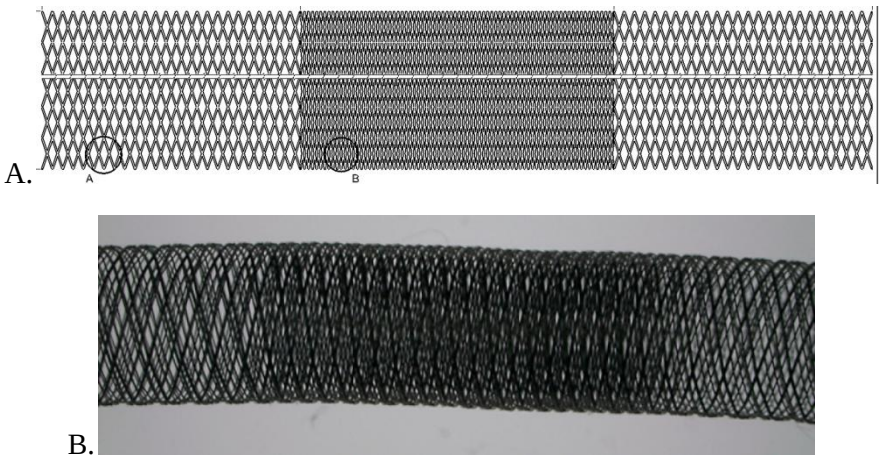

Figure 3. Schematic diagram and image of the 32-strand flow diverter configuration

This stent contains 32 nitinol wires, 4 of which are equipped with platinum wire to enhance overall visibility. The mid segment of the stent has tight braiding distances.

To reveal diverse intra-aneurysmal healing process, we designed two different flow diverters, 32- and 48-strand braided stents, which have different profiles at the nominal diameter and would provide different flow diversion effect on the similarly made aneurysms (Table 1). The stent profile was

described using porosity, or the ratio of the metal free surface area to the total surface area (pore per inch, PPI), which is defined as the number of pores per unit length of the stent. This value represents the pore density and pore size, which is defined as the area of a pore (mm^2). Both configurations had an open device diameter of 4mm or 5mm, and an open device length of 30mm. Compared with commercially available flow diverter stent, e.g. Pipeline embolization device (PED, ev3 Endovascular Inc/Covidien, Plymouth, MN, USA), and Silk (Balt Extrusion, Montmorency, France), newly designed FD shows lower porosity and PPI at the mid-segment of stent (77.2 ± 2.9%, 70.4 ± 1%, 64.1% of 32-strand FD, and 55.4% of 48-strand FD; 128, 144, 61 of 32-strand FD, and 55.4 of 48-strand FD, respectively). Mid-segment pore size of newly designed FD stent is similar to PED and Silk FD stent (0.04 mm^2 of 32-strand FD, 0.03 mm^2 of 48-strand FD, 0.02-0.05mm^2, and 0.01-0.03 mm^2, respectively). The self-expanding FD is packaged pre-loaded into the 0.49 microcatheter delivery system in its elongated form with 3cm tip guide microwire.

Table 1. Flow diverter profiles.

	32-strand		48-strand	
	mid	end	mid	end
Pore size (mm^2)	0.04	0.13	0.03	0.08
Porosity (%)	64.1	80.3	55.4	77.8
PPI[1]	61	123	76	153

[1] PPI = pore per inch

3. Stent implantation

After allowing sufficient time for an aneurysm to mature (approximately 4 weeks), FDs were implanted at the aneurysms. Treated animals were given 50mg of aspirin and 37.5mg of clopidogrel orally once a day beginning 7 days before the procedure and continuing until 12 weeks after the procedure. The same anesthesia as described for aneurysm creation was employed for stent implantation. After surgical exposure of the right common femoral artery using sterile technique, a 6F vascular sheath was introduced into the vessel. Heparin (100U/kg) was administered intravenously. Under fluoroscopic guidance, a 6F guiding catheter (Envoy, Cordis Neurovascular Systems, Miami Lakes, FL) was advanced into the CCA. A roadmap image was then obtained to identify the exact location of the aneurysm neck. The pre-loaded FD system was advanced until the mid-segment covered the aneurysm neck. To achieve optimal wall apposition of FD and flow modification augmentation, the pillowed FD is released by pushing the transport wire while gently retrieving the microcatheter at the same time. Next, the whole system was appropriately pushed up. These maneuvers are repeated during the

procedure to achieve optimal deployment. The choice of device between two different FDs to be implanted in any given animal was solely dependent on the study schedule and was otherwise arbitrary.

4. Angiographic evaluation, follow-up and sacrifice of the animals

Analysis of aneurysm size was performed using linear measurements, i.e. maximal diameter and dome-to-neck ratio, obtained using the working projection and geometric comparison with reference vessel or a 10mm round metal marker. [16]

To audit the immediate outcomes of aneurysms treated with FD, intra-aneurysmal flow modification was classified as complete stasis (if no contrast media entered an aneurysm following deployment of the FD), significant flow reduction (if contrast stagnation was seen within an aneurysm in the late venous phase of the angiographic series), or slow flow (if the contrast circulation within an aneurysm became slower but without contrast stagnation in the late venous phase images) (Figure 4).[17]

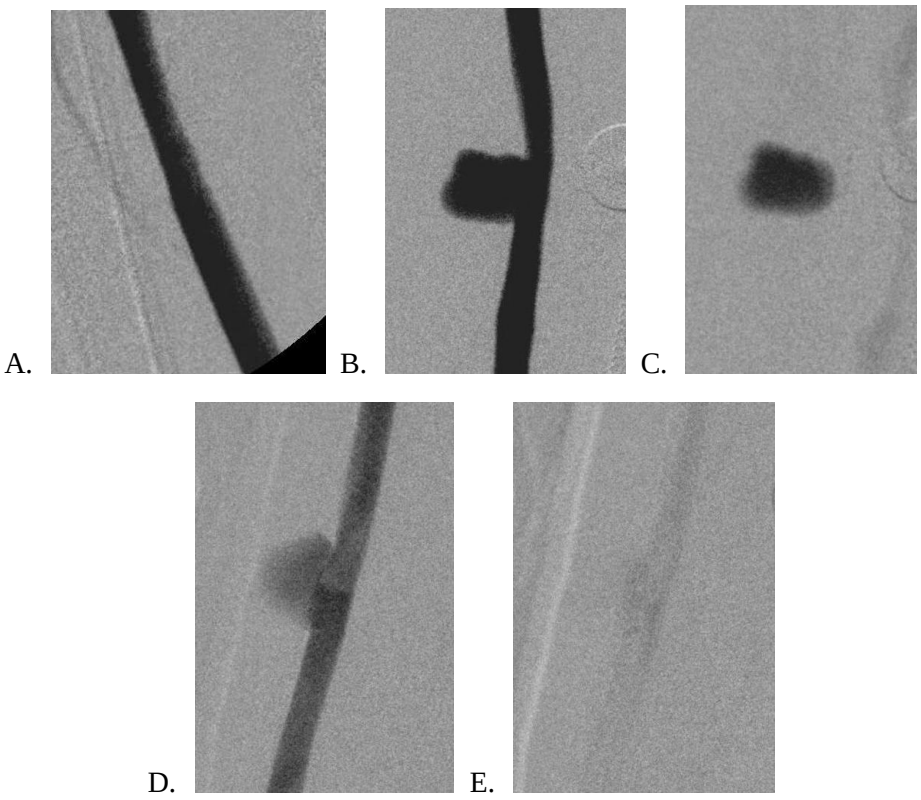

Figure 4. Intra-aneurysmal flow modification measure

A. *Complete stasis*. No contrast media entered into an aneurysm. B, C. *Significant flow reduction*. Intra-aneurysmal contrast filling was shown in the early arterial phase of the angiographic series (B), and contrast stagnation was seen within an aneurysm in the late venous phase (C). D, E. *Slow flow*. Contrast circulation within an aneurysm became slower in arterial phase of the angiographic series (D), however, contrast stagnation was not seen within an aneurysm in the late venous phase (E).

Animals were followed-up at 4 weeks (n=13, 5 animals) and 12 weeks (n=8, 3 animals) after FD implantation. Follow-up angiograms were acquired via transfemoral access as described above. Immediate and follow-up angiographic outcomes were analyzed using a five-point grading scheme as follows: grade 0, no intra-aneurysmal flow change; grade I, residual aneurysmal contrast filling ≥ 50%; grade II, residual aneurysmal contrast filling < 50%; grade III, residual contrast filling confined to the neck region; grade IV, no residual contrast filling (Figure 5).[18] Two observers analyzed all angiographic data, and consensus was reached by means of discussion in cases of discrepancy.

Under deep anesthesia induced with ketamine (50mg/kg) and Rompun (10mg/kg), the animal was euthanized with an intravenous administration of potassium chloride after final angiographic follow-up. The aneurysm-parent artery complex was then explanted and flushed with normal saline and 10% formalin.

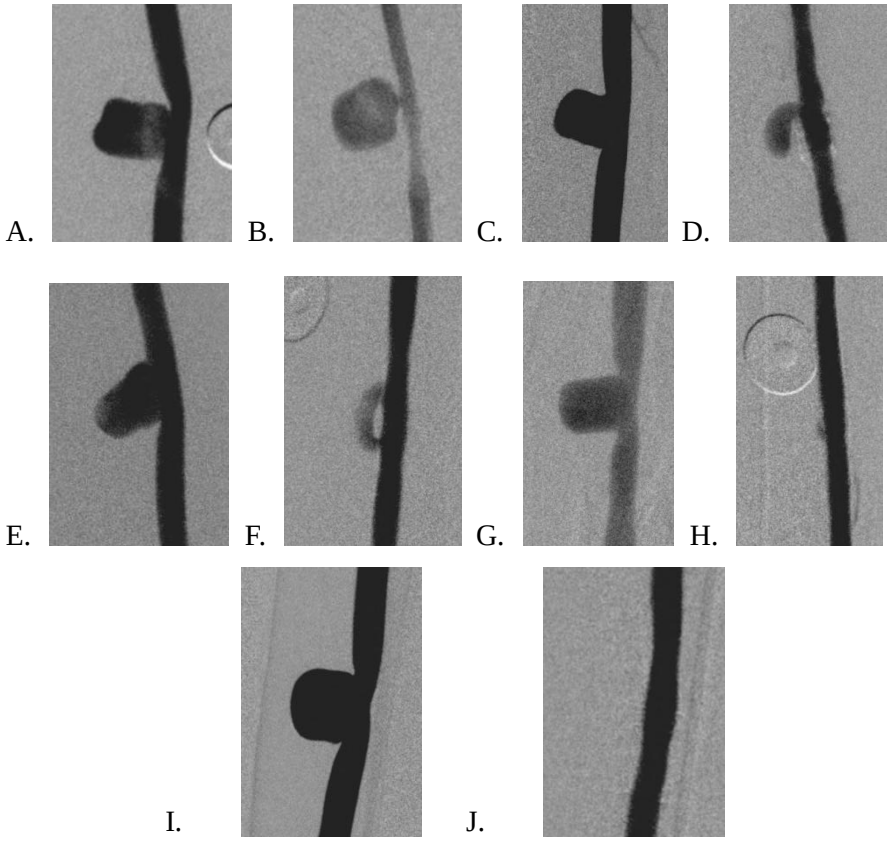

Figure 5. Angiographic outcome measure

A, B. *Grade 0*. No intra-aneurysmal flow change between pre-procedural (A) and follow-up angiography (B). C,D. *Grade I*. Residual aneurysmal contrast filling ≥ 50% between pre-procedural (C) and follow-up angiography (D). E,F. *Grade II*. Residual aneurysmal contrast filling < 50% between pre-procedural (E) and follow-up angiography (F). G, H. *Grade III*. Residual contrast filling confined to the neck region of follow-up angiography (H). I, J. *Grade IV*. No residual contrast filling follow-up angiography (J).

5. Tissue processing

The formalin-fixed tissue samples were processed through a graded series of ethanol and xylene, and were embedded in methyl-methacrylate (MMA). Three representative cross sections per stented segment (proximal, middle, and distal) for the 14 early aneurysms and one longitudinal section for the 7 late aneurysms were taken from the block at approximately 600 μm intervals, polished down to 6 μm, and stained with hematoxylin-eosin (H-E) stain.

Morphometric measurements were performed as follows: thickness of neointima = distance between the outer surface of stent strut and the luminal border at the thickest area; neolumen = distance from luminal border to luminal border; former vessel lumen = distance from the outside of a strut to the opposite outside of the strut across the vessel diameter; diameter stenosis = (neolumen/former lumen) X100 at the narrowest neoluminal area. (Figure 6)

A. 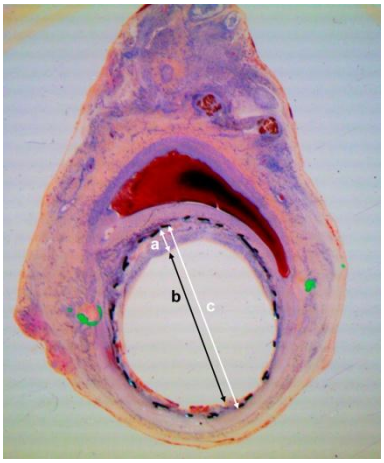

B. 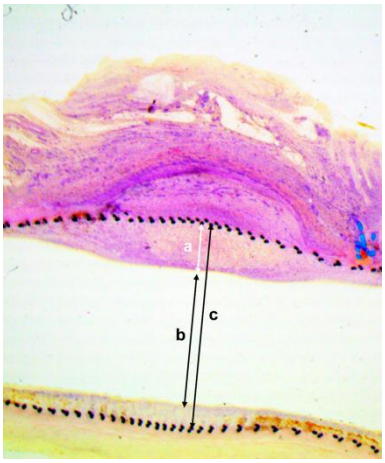

Figure 6. Morphometric measures of neointima, neolumen and former vessel lumen

a indicates a neointima; b, neolumen; and c, former vessel lumen on the cross (A) and longitudinal (B) sectional slide.

6. Statistical analysis

Angiographic outcomes were compared between the two different FD groups, 32-strand stent and 48-strand stent, to evaluate the degree of flow diversion. We analyzed angiographic aneurysmal dimensions using a 2-way analysis of variance (ANOVA; stent*follow-up duration).

The chi-square test was used to compare the frequency distributions of categorical variables between the study groups. Continuous variables were analyzed by the Mann-Whitney U test. Probability values of less than 0.05

were regarded as statistically significant. All statistical analyses were performed with SPSS 17.0 software for Windows (SPSS Inc., Chicago, IL).

III. RESULTS

1. Angiographic findings

All of surgically created 24 aneurysms remained patent during a follow-up period of 4 weeks. Among these, 21 aneurysms were used for FD deployment. Two-way ANOVA revealed no interaction between the two groups for width, neck size, depth, or dome-to-neck ratio of an aneurysm (Table 2). If the main effect “stent” was examined and all time points were grouped together, there were no differences in width (9.1 ± 0.6 mm vs. 9.7 ± 0.5 mm; $p = 0.41$), neck size (8.5 ± 0.5 mm vs. 9.0 ± 0.5 mm; $p = 0.44$), depth (8.0 ± 0.7 mm vs. 7.6 ± 0.6 mm; $p = 0.66$), or DN ratio (0.9 ± 0.1 mm vs. 0.9 ± 0.1 mm; $p = 0.38$) for aneurysms treated with the 32-strand versus 48-strand stent, respectively. After all, there are no significant differences in aneurysmal geometry between two different group of follow-up periods and FD specifications.

In all cases, the delivery and deployment of the devices were successful without periprocedural complications. Nine of 32-strand FDs and 12 of 48-

Table 2. Aneurysm description by duration with 32-strand and 48-strand flow diverter stent

Follow-up (weeks)	Width (mm)		Neck (mm)		Depth (mm)		DN ratio	
	32-strand	48-strand	32-strand	48-strand	32-strand	48-strand	32-strand	48-strand
4	9.4 ± 0.8	10.1 ± 0.6	8.8 ± 0.7	9.0 ± 0.5	8.0 ± 0.9	8.9 ± 0.7	0.9 ± 0.1	1.0 ± 0.1
12	8.8 ± 0.9	9.4 ± 0.9	8.1 ± 0.7	9.0 ± 0.7	8.0 ± 1.1	6.3 ± 1.1	1.0 ± 0.1	0.7 ± 0.1
p value	0.92		0.57		0.19		0.09	

strand FDs were deployed at each an aneurysm. The same type of FDs was usually deployed at each dog except 2 dogs harboring 4 and 2 aneurysms of each.

Table 3 summarizes angiographic outcomes. After placement of the FD, complete control angiogram showed significant flow reduction in 11 aneurysms and slow flow in 10 aneurysms. There was no difference in flow modification between the two groups (p = 0.67; 2-tailed Fisher's Exact test). In accordance with the 5-point grading scheme, overall occlusion rates of grade 0, I, and II were noted in 9 (42.9%), 10 (47.6%), and 2 (9.5%) of 21

aneurysms, respectively. There was no difference in the immediate angiographic occlusion rate between the two groups (p = 0.32; 2-tailed Fisher's Exact test).

At 4 weeks follow-up, angiography revealed 2 (22.2%) versus 0 grade 0, 3 (33.3%) versus 0 grade I, 3 (33.3%) versus 5 (41.7%) grade II, 0 versus 3 (25.0%) grade III, and 1 (11.2%) versus 4 (33.3%) grade IV aneurysms for groups treated with the 32-strand versus 48-strand stent, respectively. Aneurysms treated with the 48-strand FD showed a higher occlusion rate compared with aneurysms treated with the 32-strand FD (p for trend = 0.009). Flow modification was not associated with aneurysmal occlusion rate at 4-week follow-up (p for trend = 0.18). On the other hand, a higher grade immediate angiographic occlusion rate was significantly associated with higher grade occlusion rate at 4-week follow-up (p for trend = 0.008).

At 12 weeks, follow-up angiograms revealed 1 (25.0%) versus 0 grade 0, 2 (50.0%) versus 0 grade I, 1 (25.0%) versus 0 grade II, 0 versus 1 (25.0%) grade III, and 0 versus 3 (75.0%) grade IV aneurysms treated with 32-strand

versus 48-strand stents, respectively. Aneurysms treated with the 48-strand FD showed a higher occlusion rate compared with aneurysms treated with the 32-strand FD (p for trend = 0.029). Flow modification and immediate angiographic occlusion rate were not associated with the occlusion rate at 12-week follow-up (p for trend = 0.59 and 0.13, respectively).

Table 3-1. Angiographic outcomes of aneurysms treated with 32-strand flow diverters

Aneurysm No.	Flow modification	Immediate outcome	4 weeks follow-up	12 weeks follow-up
1	slow flow	I	I	II
2	slow flow	0	I	I
3	significant flow reduction	0	I	I
4	significant flow reduction	0	0	0
8	slow flow	I	II	
9	significant flow reduction	I	II	
15	slow flow	I	IV	
16	significant flow reduction	0	II	
21	significant flow reduction	0	0	

Table 3-2. Angiographic outcomes of aneurysms treated with 48-strand flow diverters

Aneurysm No.	Flow modification	Immediate outcome	4 weeks follow-up	12 weeks follow-up
5	slow flow	I	IV	
6	slow flow	I	II	
7	significant flow reduction	0	II	
10	slow flow	0	II	
11	slow flow	0	II	IV
12	slow flow	I	II	IV
13	significant flow reduction	I	IV	IV
14	significant flow reduction	0	III	III
17	significant flow reduction	I	IV	
18	slow flow	I	III	
19	slow flow	II	IV	
20	slow flow	II	III	

2. Histopathologic findings

Four of 9 aneurysms treated using 32-strand FD was harvested at 12-week follow-up, and the other 5 aneurysms were harvested at 4-week follow-up. Four of 12 aneurysms treated using 48-strand FD was harvested at 12-week follow-up, and the other 8 aneurysms were harvested at 4-week follow-up.

At 4 weeks, intra-aneurysmal histopathologic findings of completely occluded aneurysms (grade IV) were variable (Table 4-3). Cross sections of an aneurysm 5 show that the aneurysmal sac was filled with concentrically laminated thrombi of various stages of organization (Figure 7-C, D, E). The thrombi of an aneurysm 19 revealed irregular, ill-defined laminations primarily composed of organized thrombus (Figure 7-F). Midline longitudinal sections of aneurysms 15 and 17 showed significantly shrunken aneurysmal sacs, and a small area of organized thrombus and attenuated cellular matrix with thick neointima formation (Figure 7-G).

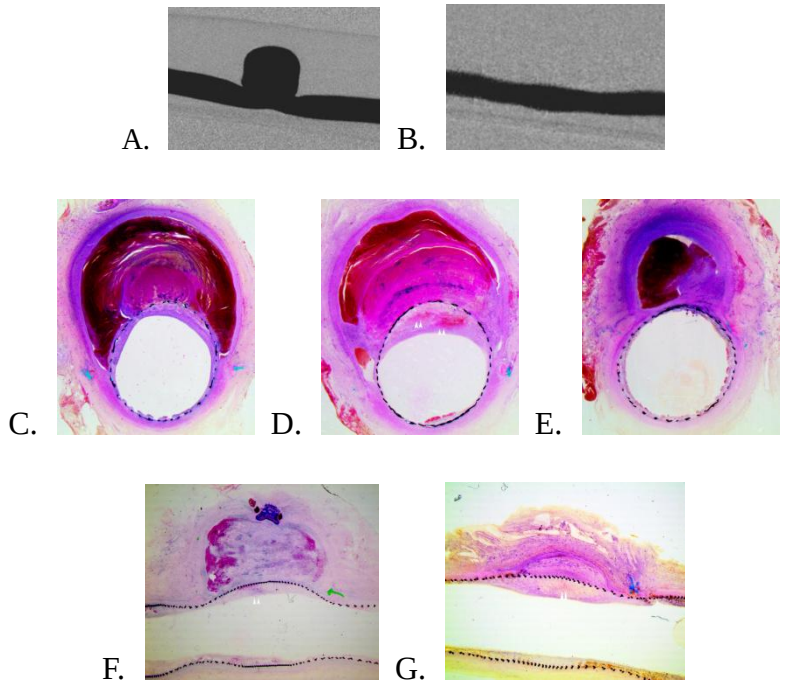

Figure 7. Aneurysms of complete occlusion at 4-week follow-up

A. Pre-procedural common carotid arteriogram shows a large, wide-necked side wall aneurysm (an aneurysm 5) B. 4 week follow-up angiograph of an aneurysm 5 shows complete occlusion. C-E. Photomicrographs of an aneurysm 5. Proximal (C), mid (D), and distal (E) segment of cross sections shows multi-staged thrombus formation in a concentrically laminated fashion. F. Midline longitudinal section of an aneurysm 19 shows thrombi with irregular, ill-defined laminations primarily composed of organized thrombus. G. Midline longitudinal section of aneurysm 15 shows a significantly shrunken aneurysmal sac, and a small area of organized thrombus and attenuated cellular matrix with neointimal hyperplasia around the aneurysmal neck. Neointimal hyperplasia was present in the mid-segment of an aneurysm, containing organized thrombus (*arrowheads*, D, F, and G).

Aneurysms with near occlusion (grade III) also demonstrate diverse findings (Table 4-2). A midline longitudinal section of an aneurysm 20 showed that the aneurysmal sac was filled with laminated thrombus of various stages of organization (Figure 8-C). Aneurysm 18 was shrunken in size, and fresh blood clot surrounded by organized thrombus was present. The distance between stent struts was relatively wide at the segment proximal to the fresh blood clot (arrowheads, Figure 8-F) compared with other segments. The aneurysmal sacs of incompletely occluded aneurysms (grade 0 – II) were usually filled with multi-staged thrombus primarily composed of a fresh blood clot with or without a small empty space (Figure 9-E, F,) (Table 4-1 and 4-2). A paramedian longitudinal section of an aneurysm 16 showed a small amount of organized thrombus formation around stent struts with an intimal defect (Figure 9-I).

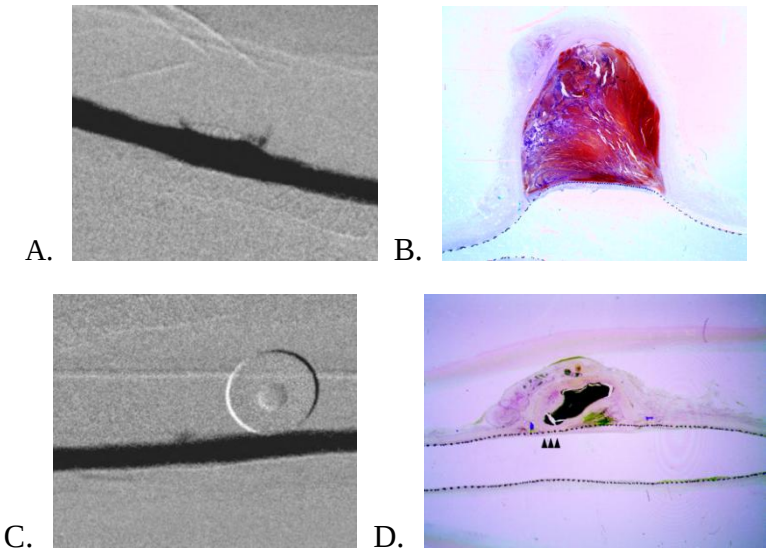

Figure 8. Aneurysms of grade III occlusion at 4-week follow-up

A. 4-week follow-up angiograph of an aneurysm 20 shows near complete occlusion (grade III). C. Midline longitudinal section of an aneurysm 20 shows the aneurysmal sac filled with laminated thrombus at various stages of organization. C. 4-week follow-up angiograph of aneurysm 18 shows near complete occlusion (grade III). D. Midline longitudinal section of an aneurysm 18 shows that it has shrunken in its size, and fresh clot surrounded by organized thrombus is present. The distance between stent struts was relatively wide at the segment near the fresh blood clot (*arrowheads*, D) compared with other segments.

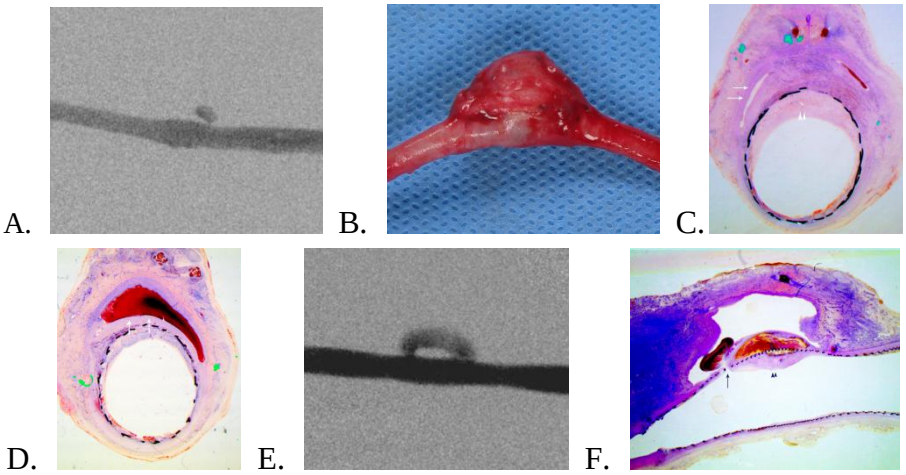

Figure 9. Aneurysms of incomplete occlusion at 4-week follow-up

A. 4-week follow-up angiograph of an aneurysm 9 shows incomplete occlusion (grade II). B. Four weeks after stent implantation, the aneurysm has shrunken in size. C, D. Photomicrographs of an aneurysm 9. Mid (C) and distal (D) segments of cross sections show that the aneurysmal sac was filled with multi-staged thrombus primarily composed of a fresh blood clot (*arrows*, D) with small empty space (*arrows*, C). E. 4-week follow-up angiograph of an aneurysm 16 shows incomplete occlusion (grade II). F. Paramedian longitudinal section of an aneurysm 16 shows a small amount of organized thrombus along the stent strut with the intimal defect (*arrow*, F). A small amount of fresh blood clot is adjacent to the intimal defect with a large empty space within the aneurysmal sac. Neointimal hyperplasia is present in the mid-segment of an aneurysm, containing organized blood clot (*arrowheads*, C and F).

At 12 weeks, grade IV aneurysms were significantly shrunken, and histopathology showed a small area of organized thrombus and attenuated cellular matrix with a thin neointima (Figure 10 A, B) (Table 5-2). Grade III aneurysms were also significantly shrunken in size, and histopathology showed a small area of organized thrombus and attenuated cellular matrix with small amounts of an unorganized blood clot (Figure 10 C, D) (Table 5-2). Incompletely occluded aneurysms (grade 0 – II) most commonly showed empty sacs with small amounts of variably organized thrombus formation at the fringe neck formed between the aneurysmal wall and stent struts in coronal sections with large empty spaces within the aneurysmal sac (Figure 11) (Table 5-1).

A. 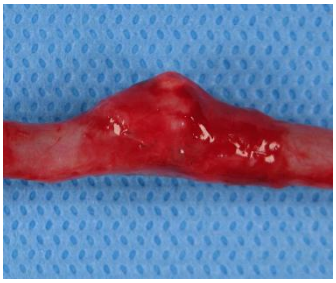 B. 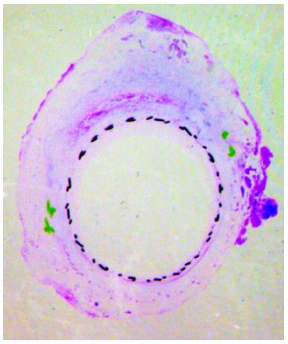

C. 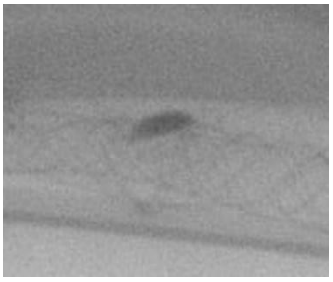 D. 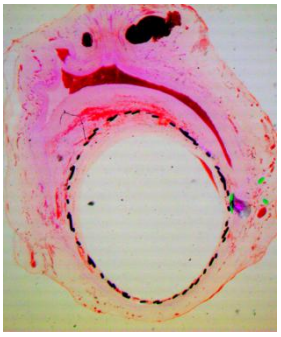

Figure 10. Aneurysms of complete and grade III occlusion at 12-week follow-up

A. Gross inspection of completely occluded aneurysm 13 (grade IV). It is significantly shrunken in size. B. Photomicrographs of the mid-segment of coronal sections (aneurysm 13). The aneurysmal sac is significantly shrunken, and histopathology shows a small area of organized thrombus and attenuated cellular matrix with a thin neointima. C. Native plane radiograph of an aneurysm 14 obtained immediately after 12-week follow-up angiography, showing a small amount of contrast stagnation at the aneurysmal neck (grade III). D. Photomicrographs of an aneurysm 14. Mid-segment of the coronal section shows a significantly shrunken aneurysmal sac, and a small area of sharp, crescentic fresh blood clot and attenuated cellular matrix with a thin neointima.

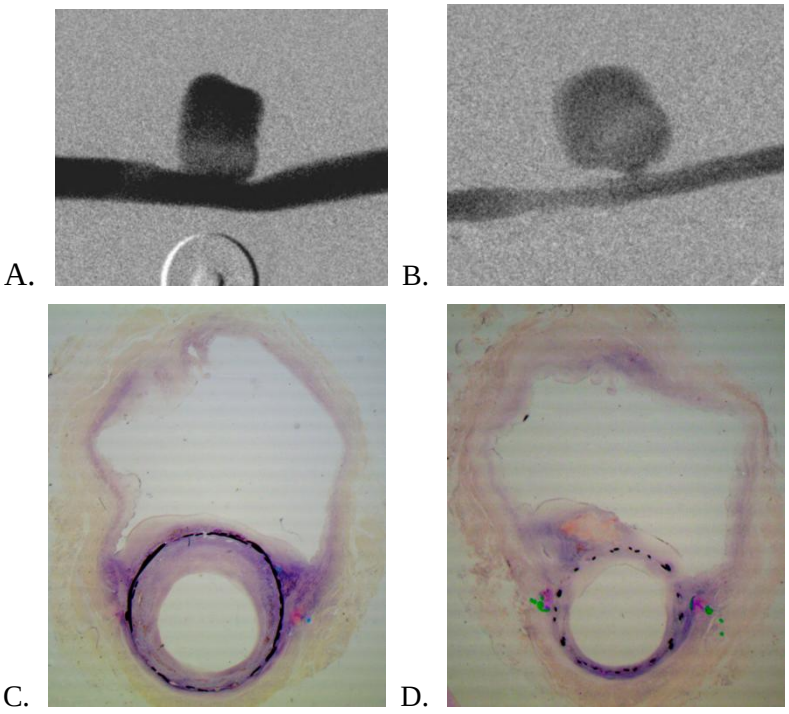

Figure 11. Aneurysm of incomplete occlusion at 12-week follow-up

A. Pre-procedural common carotid arteriogram shows a large, wide-necked side wall aneurysm (aneurysm 4) B. 12-week follow-up angiograph of an aneurysm 4 shows incomplete occlusion, and neointimal formation with the intimal defect at the distal segment of the aneurysmal neck. C, D. Photomicrographs of an aneurysm 4. Proximal (C) and mid (D) segments of cross sections show an empty sac with a small amount of variably organized thrombus at the fringe neck formed between the aneurysmal wall and stent struts with intimal hyperplasia at the proximal segment of the aneurysm.

Neointimal thickness and diameter stenosis was not significantly different between 4-week and 12-week follow-up, but showed a decreasing tendency after 12 weeks in completely occluded aneurysms (0.99 ± 0.57mm vs. 0.53 ± 0.14mm, *p* value = 0.16; 29.6 ± 8.36mm vs. 13.1 ± 3.54mm, *p* value = 0.69). In contrast, neointimal thickness and diameter stenosis showed an increasing trend after 12 weeks in near complete (0.84 ± 0.34mm vs. 0.97 ± 0.43mm, *p* value = 0.78; 17.2 ± 6.52mm vs. 19.0 ± 26.1mm, *p* value = 0.91) and incomplete (0.94 ± 0.29mm vs. 1.13 ± 0.59mm, *p* value = 0.49; 23.1 ± 5.03mm vs. 39.9± 7.16mm, *p* value = 0.16) occluded aneurysms. Neointimal thickness and diameter stenosis between groups treated with 32-strand and 48-strand FDs were not significantly different (1.01 ± 0.37mm vs. 0.81 ± 0.39mm, *p* value = 0.82; 30.2 ± 11.1mm vs. 17.8 ± 8.31mm, *p* value = 0.34).

Table 4-1. Angiographic outcomes and histopathologic findings at 4-week follow-up.

Aneurysm No.	Angiographic outcome	Histopathology		
		Proximal	Mid	Distal
21	0		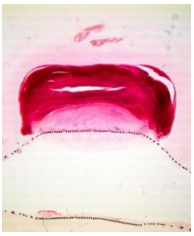	
6	II	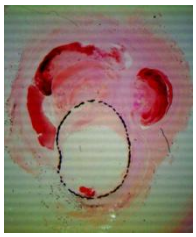	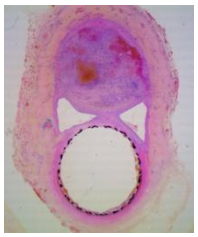	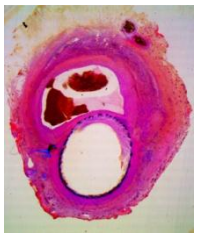
7	II	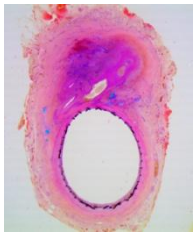	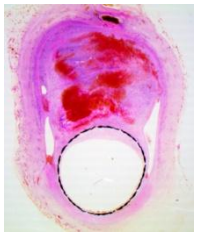	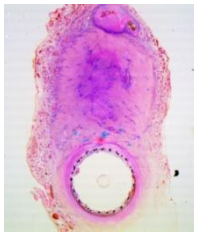
8	II	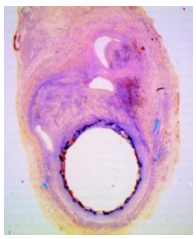	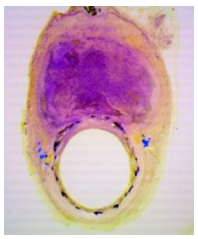	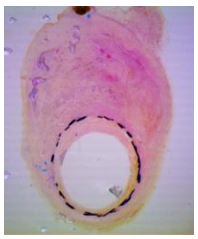
9	II	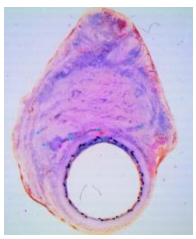	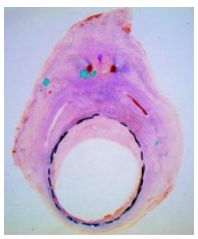	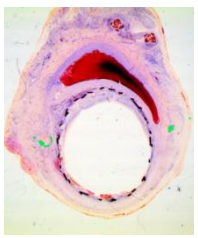

Table 4-2. Angiographic outcomes and histopathologic findings at 4-week follow-up.

Aneurysm No.	Angiographic outcome	Histopathology		
		Proximal	Mid	Distal
10	II	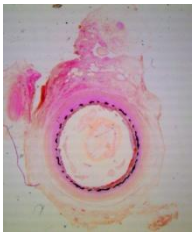	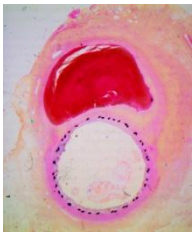	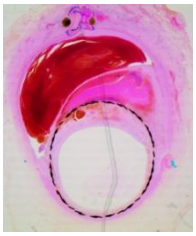
16	II		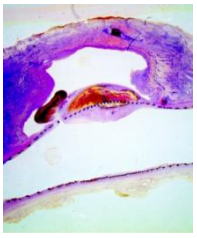	
18	III			
20	III		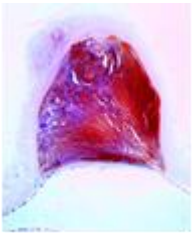	

Table 4-3. Angiographic outcomes and histopathologic findings at 4-week follow-up.

Aneurysm No.	Angiographic outcome	Histopathology		
		Proximal	Mid	Distal
5	IV	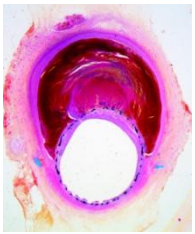	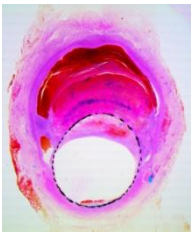	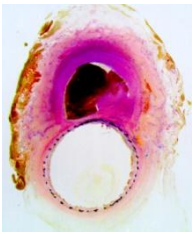
15	IV		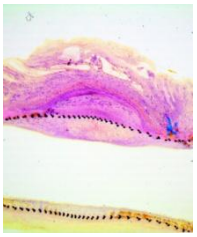	
17	IV		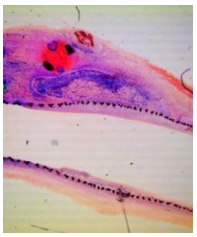	
19	IV		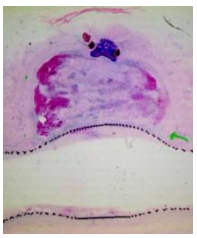	

Table 5-1. Angiographic outcomes and histopathologic findings at 12-week follow-up.

Aneurysm No.	Angiographic outcome	Histopathology		
		Proximal	Mid	Distal
4	0	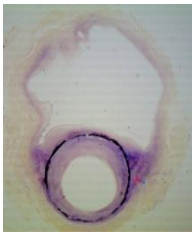		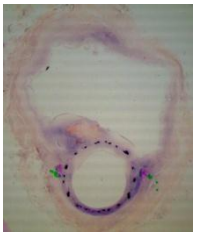
2	I	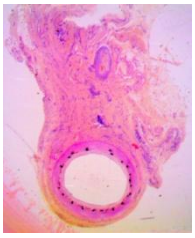	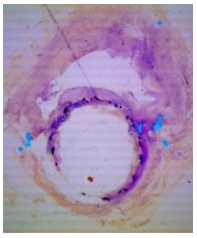	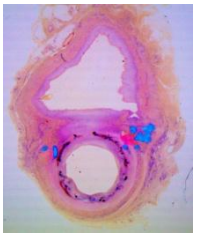
3	I	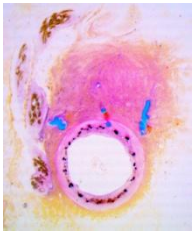	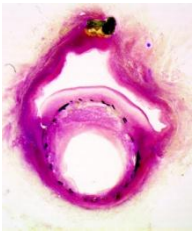	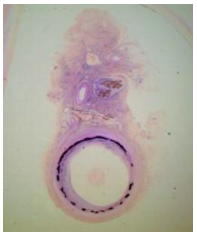
1	II	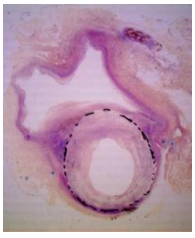	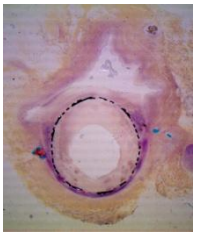	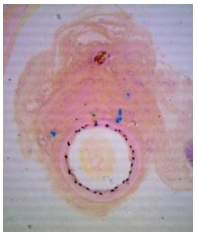

Table 5-2. Angiographic outcomes and histopathologic findings at 12-week follow-up.

Aneurysm No.	Angiographic outcome	Histopathology		
		Proximal	Mid	Distal
14	III	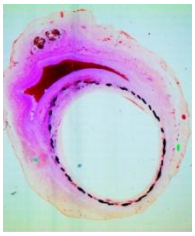	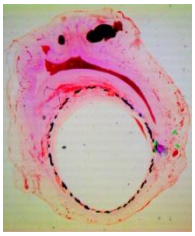	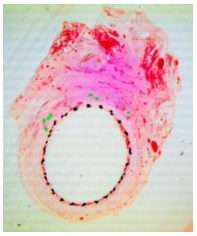
11	IV	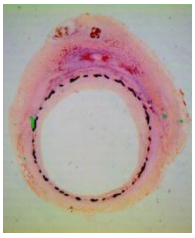	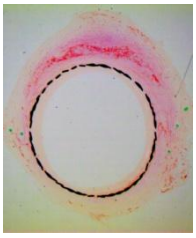	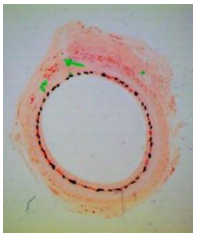
12	IV	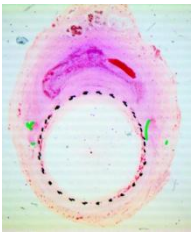	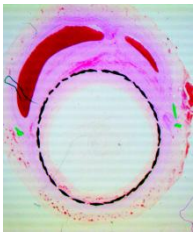	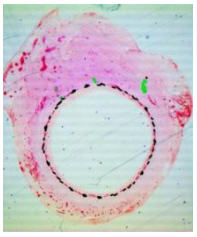
13	IV	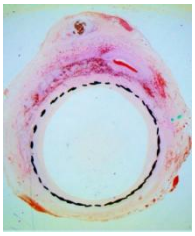	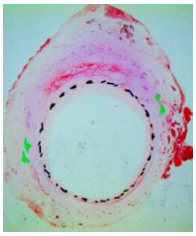	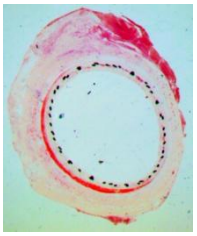

IV. DISCUSSION

The present study reveals various histopathologic findings in aneurysms treated with the same type of FD showing same angiographic outcomes at a specific follow-up period. However, the neointimal formation was observed in all aneurysms along the stent struts.

Numerous experimental studies have been performed to evaluate healing process of aneurysms treated using FD. Mostly, it focused on the efficacy of FD or degree of hemodynamic alteration induced by FD, and histopathologic findings were concomitantly presented.[8-13] Hence, exact progression of intra-aneurysmal thrombus formation after FD deployment was not clearly understood. Some authors demonstrated the process of neointimal formation in term of aneurysm healing after FD deployment.[14, 15] However, there are some limitations to our comprehension of the overall aneurysm healing process. We surgically made side wall aneurysms similar in terms of geometry, and it would provide similar intra-aneurysmal hemodynamics. We designed

two different type of FD to induce different flow diversion effect, and compared angiographic outcomes with histopathologic findings at a specific follow-up period.

According to various experimental data on intra-aneurysmal hemodynamics, FDs disrupt the vortical flow of aneurysms and decreases the inflow rate.[19-22] As a result, intra-aneurysmal thrombosis is induced by the modified local hemodynamic conditions. In particular, sidewall aneurysm hemodynamic studies revealed that the intra-aneurysmal vortex after FD implantation starts at the distal neck and flows along the aneurysmal wall, with flow stagnation more prominent at the proximal segment of an aneurysm and proximal to the mid-segment of the neck. Our histopathologic findings support this hypothesis. Intra-aneurysmal thrombi were formed in a laminated pattern in completely and near-completely occluded aneurysms at 4-weeks follow-up, with various stages of organization (Figures 7 & 8). The presence of a laminated thrombus implies thrombosis at the site of blood flow, which means thrombus formation progresses gradually along the direction of flow.[23] Figure 8-B showed an

intra-aneurysmal thrombus with laminations, and the pattern of lamina resembles the flow direction of the intra-aneurysmal vortex after FD deployment. Figure 7-C and D show a relatively more organized thrombus formed around the proximal- and mid-segment of the aneurysmal neck area. Histopathologic findings of incompletely occluded aneurysms revealed that organized thrombus was present at the neck area or a fringe neck formed between the aneurysmal wall and stent struts, with a fresh blood clot or empty space in the aneurysmal dome (Figures 9-C and D, 10-D, 11-D). These locations where more organized thrombi were observed would represent hemodynamically inert areas immediately after FD deployment, as previously demonstrated in *ex-vivo* experimental data.[24, 25] According to these findings, we hypothesized that each layer of an organized thrombus would be gradually formed at different time points along the newly induced intra-aneurysmal flow associated with the FD.

Angiographic outcomes reveal that the 48-strand FD achieved a higher occlusion rate compared with the 32-strand FD, and immediate angiographic

outcomes were positively associated with 4-week angiographic outcomes. Higher pore density and metal coverage usually induce a higher flow diversion effect.[8, 12] Overall, the degree of intra-aneurysmal hemodynamic alteration induced by the FD affects immediate intra-aneurysmal thrombus formation. The more thrombus occupying a portion of the aneurysmal sac, the less intra-aneurysmal flow achieved. Eventually, it would lead to diverse histopathologic findings of aneurysms corresponding to equivalent angiographic outcomes at specific follow-up period.

We supposed that relatively similar pattern of intra-aneurysmal histopathologic findings in aneurysms treated using a particular specification of FD at specific follow-up period. However, various degrees and patterns of intra-aneurysmal thrombus formation with different sized aneurysm sacs were found among aneurysms treated using the same type of FD and showing the same angiographic outcomes at a specific follow-up period, (Figures 7, 8 and 9). Histopathologic findings of an aneurysm 18 and 16 show the proximity of fresh blood clot or neointimal defect with a small amount of

fresh blood clot at the segment where the distance between stent struts was relatively wide (Figure 8-D and 9-F). Active inflow could remain through the segment, and it might disrupt stable intra-aneurysmal thrombus formation. In addition, active inflow into the aneurysmal sac could interrupt neointima formation by disturbing muscle and endothelial cell migration along the stent strut, and it could augment intra-aneurysmal flow. Using FD to treat an aneurysm arising from the convex side of parent artery, the distance between stent strut could be widened at the neck of an aneurysm. In these cases, it could adversely affect aneurysm healing. In addition, inherent thrombogenicity and degree of antiplatelet response might be associated with these histopathologic findings (Figure 7, 8 and 9). Following intra-aneurysmal thrombus formation induced by the FD, the thrombus is replaced by organized connective tissue. In sequence, this would lead to shrinkage of an aneurysm to various degrees.[26] Altered size and geometry of an aneurysm would lead to additional intra-aneurysmal hemodynamic changes. After all, individual-specific thrombogenicity and the antiplatelet response would also be

associated with gradual alteration of intra-aneurysmal hemodynamics to promote aneurysm healing. Heterogeneity of thrombogenicity and the antiplatelet response is well known,[27] and this might also result in a greater or lesser degree of thrombus formation and organization. These biologic factors might influence the dynamic intra-aneurysmal hemodynamic changes after FD deployment.

After FD deployment to treat aneurysms, a degree of aneurysm healing is usually evaluated using angiographic findings. And, we presumed that histopathologic findings of aneurysms after FD deployment would be relatively homogenous depending on degrees of an angiographic outcome. However, the present study revealed diverse histopathologic findings of aneurysms show the same degree of angiographic outcomes. With regard to these findings, the angiographic outcome could not represent a degree of aneurysm healing after FD deployment.

Neointimal formation of variable thickness was observed in all aneurysms treated with FD, and there was no significant difference between the groups

treated with two different FDs. Kadirvel et al. demonstrated that endothelialization is exclusively derived from cells in the adjacent parent artery, and smooth muscle and endothelial cells grow over the struts of the device itself.[14] Regardless of stent specification, it is supposed that struts of the FD act as scaffolds for neointimal formation. In addition, neointimal formation seems to be independent of intra-aneurysmal thrombus formation. Histopathologic findings of an aneurysm 4, which shows grade 0 occlusion at 12-week follow-up, support this hypothesis. This aneurysm showed thick neointima formation with a large empty space in the intra-aneurysmal sac and a scant amount of intra-aneurysmal thrombus formation (Figure 11-C, D). Some authors suggested that neointimal formation is more important than intra-aneurysmal thrombus formation in the complete occlusion of aneurysms.[14, 15] In accordance with these findings, however, we hypothesize that neointimal formation is an independent process to intra-aneurysmal thrombus formation, and complete occlusion of an aneurysm could not be achieved without intra-aneurysmal thrombus formation .

Our study has several limitations. First, we use canine venous pouch aneurysm models. Compared with the elastase-induced arterial aneurysm model, it is less physiologically accurate.[28] Hence, it was unrealizable to simulate delayed aneurysmal rupture after FD deployment. However, currently available, various animal models present multiple weaknesses in term of implementation of real aneurysms of human.[29] Using canine venous pouch aneurysm models, we were able to create relatively consistent-sized aneurysms that provided similar intra-aneurysmal hemodynamics. In addition, the lack of spontaneous thrombosis or rupture[30] is valuable for the evaluation of histopathologic changes within the aneurysms induced only by FDs without any unexpected events. Second, even though we recognize inherent thrombogenicity and the antiplatelet response as independent factors associated with aneurysmal healing, we could not evaluate these in the present study. Based on the dogs' weight, which was around 30 kg, a half-dose of standard aspirin and clopidogrel, as prescribed for adult patients at our institute, was used. We suspect that our antiplatelet medication strategy for

experimental animals might reflect our clinical practice. Because of the difference between species and heterogeneity of the antiplatelet response, however, our findings should be interpreted carefully. Finally, the number of aneurysms included in the study is limited, especially in the 12-week follow-up group. Studies with a larger number of subjects are needed to confirm the trends observed in this experimental study. Despite these limitations, this study demonstrates the healing process of aneurysms treated using FDs by documenting histopathological changes over time. By comparing angiographic and histopathologic findings, our results provide a useful schema for the healing process of an aneurysm treated using FDs in clinical practice.

V. Conclusion

Among aneurysms showing the same angiographic outcomes at a specific follow-up period, various degrees and patterns of intra-aneurysmal thrombus formation with different sized aneurysm sacs were found. Ultimately, the angiographic outcome could not represent a degree of aneurysm healing after FD deployment. Neointimal formation could occur along the struts of the FD independently of intra-aneurysmal thrombus formation. However, neointima formation could not solely lead to complete aneurysm healing. Intra-aneurysmal thrombus formation and organization seems to be an important factor for the complete occlusion of aneurysms treated using the FD.

VI. REFERENCES

1. Arrese I, Sarabia R, Pintado R, Delgado-Rodriguez M. Flow-diverter devices for intracranial aneurysms: systematic review and meta-analysis. *Neurosurgery.* Aug;73(2):193-199; discussion 199-200.

2. Briganti F, Napoli M, Tortora F, et al. Italian multicenter experience with flow-diverter devices for intracranial unruptured aneurysm treatment with periprocedural complications--a retrospective data analysis. *Neuroradiology.* Oct;54(10):1145-1152.

3. Brinjikji W, Murad MH, Lanzino G, Cloft HJ, Kallmes DF. Endovascular treatment of intracranial aneurysms with flow diverters: a meta-analysis. *Stroke.* Feb;44(2):442-447.

4. Yu SC, Kwok CK, Cheng PW, et al. Intracranial aneurysms: midterm outcome of pipeline embolization device--a prospective study in 143 patients with 178 aneurysms. *Radiology.* Dec;265(3):893-901.

5. Chan TT, Chan KY, Pang PK, Kwok JC. Pipeline embolisation device for wide-necked internal carotid artery aneurysms in a hospital in

Hong Kong: preliminary experience. *Hong Kong Med J.* Oct;17(5):398-404.

6. Cirillo L, Dall'olio M, Princiotta C, et al. The use of flow-diverting stents in the treatment of giant cerebral aneurysms: preliminary results. *Neuroradiol J.* Apr;23(2):220-224.

7. Kallmes DF, Hanel R, Lopes D, et al. International retrospective study of the pipeline embolization device: a multicenter aneurysm treatment study. *AJNR Am J Neuroradiol.* Jan;36(1):108-115.

8. Sadasivan C, Cesar L, Seong J, et al. An original flow diversion device for the treatment of intracranial aneurysms: evaluation in the rabbit elastase-induced model. *Stroke.* Mar 2009;40(3):952-958.

9. Augsburger L, Farhat M, Reymond P, et al. Effect of flow diverter porosity on intraaneurysmal blood flow. *Klin Neuroradiol.* Aug 2009;19(3):204-214.

10. Kallmes DF, Ding YH, Dai D, Kadirvel R, Lewis DA, Cloft HJ. A second-generation, endoluminal, flow-disrupting device for treatment

of saccular aneurysms. *AJNR Am J Neuroradiol.* Jun 2009;30(6):1153-1158.

11. Cebral JR, Mut F, Raschi M, et al. Analysis of hemodynamics and aneurysm occlusion after flow-diverting treatment in rabbit models. *AJNR Am J Neuroradiol.* Aug;35(8):1567-1573.

12. Ma D, Xiang J, Choi H, et al. Enhanced aneurysmal flow diversion using a dynamic push-pull technique: an experimental and modeling study. *AJNR Am J Neuroradiol.* Sep;35(9):1779-1785.

13. Ionita CN, Natarajan SK, Wang W, et al. Evaluation of a second-generation self-expanding variable-porosity flow diverter in a rabbit elastase aneurysm model. *AJNR Am J Neuroradiol.* Sep;32(8):1399-1407.

14. Kadirvel R, Ding YH, Dai D, Rezek I, Lewis DA, Kallmes DF. Cellular mechanisms of aneurysm occlusion after treatment with a flow diverter. *Radiology.* Feb;270(2):394-399.

15. Li ZF, Fang XG, Yang PF, et al. Endothelial progenitor cells

contribute to neointima formation in rabbit elastase-induced aneurysm after flow diverter treatment. *CNS Neurosci Ther.* May;19(5):352-357.

16. Massoud T, Guglielmi G, Ji C, Vinuela F, Duckwiler G. Experimental saccular aneurysms. *Neuroradiology.* 1994;36(7):537-546.

17. Szikora I, Berentei Z, Kulcsar Z, et al. Treatment of intracranial aneurysms by functional reconstruction of the parent artery: the Budapest experience with the Pipeline embolization device. *American Journal of Neuroradiology.* 2010;31(6):1139.

18. Kamran M, Yarnold J, Grunwald IQ, Byrne JV. Assessment of angiographic outcomes after flow diversion treatment of intracranial aneurysms: a new grading schema. *Neuroradiology.* Jul 2011;53(7):501-508.

19. Barath K, Cassot F, Fasel JH, Ohta M, Rufenacht DA. Influence of stent properties on the alteration of cerebral intra-aneurysmal haemodynamics: flow quantification in elastic sidewall aneurysm models. *Neurol Res.* 2005;27 Suppl 1:S120-128.

20. Cebral JR, Mut F, Raschi M, et al. Analysis of hemodynamics and aneurysm occlusion after flow-diverting treatment in rabbit models. *AJNR. American journal of neuroradiology.* Aug 2014;35(8):1567-1573.

21. Ma D, Xiang J, Choi H, et al. Enhanced aneurysmal flow diversion using a dynamic push-pull technique: an experimental and modeling study. *AJNR. American journal of neuroradiology.* Sep 2014;35(9):1779-1785.

22. Meng H, Wang Z, Kim M, Ecker RD, Hopkins LN. Saccular aneurysms on straight and curved vessels are subject to different hemodynamics: implications of intravascular stenting. *AJNR. American journal of neuroradiology.* Oct 2006;27(9):1861-1865.

23. Lee R, Adlam D, Clelland CA, Channon KM. Lines of Zahn in coronary artery thrombus. *European heart journal.* May 2012;33(9):1039.

24. Lieber BB, Stancampiano AP, Wakhloo AK. Alteration of

hemodynamics in aneurysm models by stenting: influence of stent porosity. *Ann Biomed Eng.* May-Jun 1997;25(3):460-469.

25. Rhee K, Han MH, Cha SH. Changes of flow characteristics by stenting in aneurysm models: influence of aneurysm geometry and stent porosity. *Ann Biomed Eng.* Jul-Aug 2002;30(7):894-904.

26. Lee D, Yuki I, Murayama Y, et al. Thrombus organization and healing in the swine experimental aneurysm model. Part I. A histological and molecular analysis. *J Neurosurg.* Jul 2007;107(1):94-108.

27. Schafer AI. Genetic and acquired determinants of individual variability of response to antiplatelet drugs. *Circulation.* Aug 26 2003;108(8):910-911.

28. Kallmes D, Altes T, Vincent D, Cloft H, Do H, Jensen M. Experimental side-wall aneurysms: a natural history study. *Neuroradiology.* 1999;41(5):338-341.

29. Bouzeghrane F, Naggara O, Kallmes DF, Berenstein A, Raymond J. In vivo experimental intracranial aneurysm models: a systematic

review. *AJNR Am J Neuroradiol.* 2010;Mar;31(3):418-423.

30. Turk AS, Aagaard-Kienitz B, Niemann D, et al. Natural history of the canine vein pouch aneurysm model. *AJNR Am J Neuroradiol*. Mar 2007;28(3):531-532.

요약(국문초록)

개의 모델에서 혈류전환 스텐트에 의한 동맥류 치료과정의 조직병리학적 연구

혈류전환 스텐트는 뇌동맥류를 치료하기 위해 광범위하게 사용되고 있으며, 크기가 큰 동맥류나 거대동맥류에서도 치료결과가 좋다고 보고되고 있다. 그러나 혈류전환 스텐트에 의한 동맥류의 치료기전은 아직 잘 알려지지 않고 있다. 이에 본 연구는 개의 동맥류 모델에서 혈류전환 스텐트를 설치한 후 얻은 조직병리학적 소견을 통해 혈류전환 스텐트에 의한 동맥류의 치료기전을 규명하고자 하였다. 8마리의 개에 24개의 동맥류를 총경동맥에 수술적으로 만들었으며, 연구를 위해 새로이 디자인된 두가지 사양의 혈류전환 스텐트(32-strand and 48-strand)를 이용하여 24개 중 21개의 동맥류를 치료하였다. 치료후 4주 및 12주 뒤 혈관조영술을 통해 치료결과를 평가하였고, 마지막 추적검사 후 스텐트가 설치된 모동맥을 포함한 동맥류를 채취하여 조직병리학적 검사를 시행하였다. 혈관조영검사상 48-strand 스텐트가 32-strand 스텐트에 비해 동맥류의 폐쇄율이 높았다. 4주째 완전히 막힌 동맥류와 거의 다 막힌 동맥류의 조직병리학적 검사상 동맥류내 혈전은 적층구조로 형성되었으며, 동맥류의 중간부분에서 신내막 형성이 가장 활발하게 관찰되었다. 혈전의 형성과 숙성정도는

다양하였으며 동맥류의 크기도 각기 달랐다. 12주에 완전히 막힌 동맥류의 조직병리학적 소견은 동맥류내 혈전이 완전히 숙성되어 결체조직으로 차 있었으며, 그 크기도 상당히 줄어들었다. 4주째 완전히 막히지 않은 동맥류의 조직병리학적 검사상 여러단계의 혈전이 동맥류 내에 형성되어 있으며 주로 신선혈전이 대부분이었다. 동맥류내에 빈 공간이 보이는 것도 있었고 관찰되지 않는 것도 있었다. 신내막 형성은 주로 동맥류의 중간부분에서 활발하게 발생하였다. 12주째 완전히 막히지 않은 동맥류의 조직병리학적 소견상 동맥류의 경부 주변에 소량의 숙성된 혈전과 활발한 신내막 형성이 관찰되었다. 대부분의 동맥류 내부는 빈 공간으로 남아있었다. 신내막 형성의 정도는 두 스텐트 그룹 및 다른 두개의 추적관찰 기간 그룹 간에 차이를 보이지 않았다. 같은 추적관찰 기간에 시행한 혈관조영술 검사상 같은 결과를 보인 동맥류들의 조직병리학적 소견은 다양했다. 결국 혈관조영술 결과만으로는 혈류전환 스텐트로 치료한 동맥류의 치료 정도를 알 수 없다. 신내막 형성은 동맥류내 혈전 형성과 독립된 현상으로 보이며, 혈류전환 스텐트의 와이어를 따라 자라나는 것으로 보인다. 그러나 신내막 형성 단독으로 동맥류를 완전히 치료할 수는 없다. 동맥류내 혈전 형성 및 숙성이 혈류전환 스텐트에 의한 동맥류 치료에 중요한 역할을 하는 것으로 보인다.

주요어: 동맥류, 혈류전환 스텐트, 조직병리학, 개의 모델

학 번: 2010-30540